Appl Microbiol Biotechnol (2012) 93:1065–1074
DOI 10.1007/s00253-011-3599-2

Coexpression of chaperonin GroEL/GroES markedly enhanced soluble and functional expression of recombinant human interferon-gamma in *Escherichia coli*

Xiao Yan · Sheng Hu · Yi-Xin Guan · Shan-Jing Yao

Received: 18 July 2011 / Revised: 25 August 2011 / Accepted: 20 September 2011 / Published online: 6 October 2011

Abstract Recombinant human interferon-gamma (rhIFN-γ) is a protein of great potential for clinical therapy due to its multiple biological activities. However, overexpressing rhIFN-γ in *Escherichia coli* was found to accumulate as cytoplasmic inclusion bodies. In this work, a system for soluble and active expression of rhIFN-γ was constructed by coexpressing chaperonin GroEL/GroES in *E. coli*. The rhIFN-γ gene was fused to a pET-28a expression vector, and rhIFN-γ was partially expressed as the soluble form following coexpression with a second vector producing chaperonin GroEL/GroES. The fermentation of recombinant *E. coli* harboring rhIFN-γ and GroEL/GroES plasmids was investigated, and the optimized conditions were as follows: culture temperature of 25°C, incubation time of 8 h, isopropyl-β-D-thio-galactoside concentration of 0.2 mM, and L-arabinose concentration of 0.5 g/L. As a result, the expression level of rhIFN-γ was improved accordingly by 2.2-fold than the control, while a significantly positive correlation was also found between the ratio of supernatant to precipitate of rhIFN-γ and the amount of chaperonin. Circular dichroism spectra, fluorescence spectra, size exclusion chromatography, and chemical cross-linking method were applied to characterize rhIFN-γ, indicating that the three-dimensional structure of rhIFN-γ was identical to that of the native rhIFN-γ. The enzyme-linked immunosorbent assay for active rhIFN-γ quantification showed that coexpression yielded 72.91 mg rhIFN-γ per liter fermentation broth. Finally, protein–protein interactions between rhIFN-γ and chaperonin were analyzed using the yeast two-hybrid system, which provided the direct evidence that chaperonin GroEL/GroES interacted with rhIFN-γ to increase the soluble expression and presented the potential in producing efficiently recombinant proteins.

Keywords Recombinant human interferon-gamma · GroEL/GroES coexpression system · Soluble expression · Protein folding · Protein–protein interactions

X. Yan · Y.-X. Guan (✉) · S.-J. Yao
Department of Chemical and Biological Engineering,
Zhejiang University,
Hangzhou 310027, People's Republic of China
e-mail: guanyx@zju.edu.cn

S. Hu
School of Biotechnology and Chemical Engineering,
Ningbo Institute of Technology, Zhejiang University,
Ningbo 315100, People's Republic of China

Introduction

Interferons (IFNs) are a family of secretory proteins with immunomodulatory properties, which can induce an antiviral state to their target cells and inhibit cell proliferation. Human interferons (hIFNs) are divided into three major classes: hIFN-α, hIFN-β, and hIFN-γ (Gray et al. 1982). As the only type II interferon, hIFN-γ is a pleiotropic cytokine primarily produced by natural killer (NK) and natural killer T (NKT) cells, and CD4 and CD8 cytotoxic T lymphocyte (CTL) effector T cells in response to antigenic stimuli (Schoenborn and Wilson 2007). It was reported that the antitumor and immunomodulatory activity of hIFN-γ were 10–100-fold higher than that of hIFN-α and hIFN-β (Blalock et al. 1980; Rubin and Gupta 1980). Clinical trials have validated the therapeutic efficacy of hIFN-γ against many types of diseases, i.e., bladder carcinoma (Giannopoulos et al. 2003), colorectal cancer (Matsushita et al. 2006), ovarian cancer (Marth et al. 2006), renal cell carcinoma (Ellerhorst et al. 1994), leukemia (Miller et al. 2009), rheumatoid arthritis (Sigidin et al. 2001), hepatitis B infections (Parvez et al. 2006), drug-resistant tuberculosis

(Suárez-Méndez et al. 2004), etc. The native hIFN-γ is composed of 143 amino acid residues with a molecular weight of 20–25 kDa. The protein is glycosylated at two sites, and the isoelectric point is 8.3–8.5. Recombinant hIFN-γ (rhIFN-γ) is a non-glycosylated 16.7 kDa protein, but it is still physiologically active (Zhang et al. 1992). The X-ray crystal structure of rhIFN-γ forms a stable homodimer constituted by two identical, antiparallel, and non-covalently bound polypeptides. Each domain consists of six tightly associated α-helices (named A, B, C, D, E, and F), no β-sheet, and a long flexible loop between helices A and B. The dimeric structure is stabilized by the intertwining of helices across the domain interface with multiple intersubunit interactions (Ealick et al. 1991).

Expressing rhIFN-γ in *Escherichia coli* was achieved about three decades ago (Gray et al. 1982). Nevertheless, for de novo protein synthesis in cells, partially folding rhIFN-γ intermediates readily self-associated into disordered aggregates driven by the hydrophobic forces that derived from the considerable hydrophobic regions, especially the highly conserved C helix. Previous studies showed that the rhIFN-γ protein was mainly expressed as inclusion bodies in *E. coli*, and additional steps were needed to refold them in vitro to recover the correct conformation (Gao et al. 2003; Jin et al. 2006; Reddy et al. 2007), which obviously raised the cost of production. Many efforts have been attempted to achieve soluble expression of rhIFN-γ in a range of alternative hosts, e.g., mammalian cells (Gray et al. 1982), *Bacillus subtilis* (Contreras et al. 2010), and *Pichia pastoris* (Hsieh 2010), as well as to express rhIFN-γ in periplasm (Hernandez et al. 2008). However, the low expression level and the long production cycle in these processes are their key problems, which forces people to resort to *E. coli* system again.

Molecular chaperones are a large and diverse family of proteins, which control both initial protein folding and subsequent maintenance in the cells, but do not contribute conformational information to the folding process (Liberek et al. 2008). Nascent polypeptides in *E. coli* very often require a complex cellular machinery of molecular chaperones and the input of metabolic energy to counteract the aggregation stress imposed by the intricate intracellular environment, i.e., the macromolecular crowding, the high local concentration of partially folding intermediates, and the lack of translational modifications. The most extensively studied chaperone system is the chaperonin GroEL/GroES. GroEL is characterized as a large, oligomeric complex composed of 14 identical subunits which together form a stacked two-chambered structure. The GroEL cage (named Anfinsen cage) assisted by the co-chaperonin GroES and ATP can provide appropriate microenvironment for the folding of substrate intermediates (Hartl and Hayer-Hartl 2002) and facilitate protein synthesis. Reconstitution of multimeric enzymes via interactions with GroEL and GroES has previously been reported for several proteins, and most of them achieved soluble expression by the coexpression of GroEL/GroES (Brusehaber et al. 2010; Kim et al. 2009; Nishihara et al. 1998). Vandenbroeck et al. (1998) indicated that the GroEL/GroES/ATP system could increase the yield of correctly refolded IFN-γ in vitro. However, there has been no report of chaperonin GroEL/GroES system on rhIFN-γ folding in vivo yet.

In this paper, GroEL/GroES coexpressing system in *E. coli* was proposed to enhance the soluble expression of rhIFN-γ. The fermentation of recombinant *E. coli* was optimized, and the structure of rhIFN-γ was detected to evaluate the effect of chaperonin GroEL/GroES on soluble expression. Finally, the yeast two-hybrid system was used to provide a direct evidence for protein–protein interactions between rhIFN-γ and chaperonin GroEL/GroES.

Materials and methods

Plasmids and bacterial strains

Plasmid pET-28a (Novagen, USA) was used for the expression of rhIFN-γ. The rhIFN-γ gene was amplified by PCR and located at downstream of the T7 promoter between the *Nco*I and *Eco*RI sites of pET-28a, and the resulting plasmid was named pET-IFN-γ (Fig. 1a). Plasmid pGro7 encoding chaperonin GroEL/GroES was purchased from Takara (Japan) (Fig. 1b), which carried an origin of replication derived from pACYC and a chloramphenicol resistance gene (Cm^r), and the chaperonin genes were located at downstream of the araB promoter (Nishihara et al. 1998). Thus, the pET-IFN-γ and pGro7 plasmids were compatible, and the expression of rhIFN-γ and chaperonin could be induced by adding isopropyl-β-D-thio-galactoside (IPTG) and L-arabinose, respectively. *E. coli* DH5α was used for the recombinant plasmids construction and *E. coli* BL21(DE3) as the host for rhIFN-γ expression.

Expression of rhIFN-γ and GroEL/GroES in *E. coli*

Plasmids of pET-IFN-γ and pGro7 were cotransformed into *E. coli* BL21 by the calcium chloride method (Sambrook et al. 1989). Recombinant *E. coli* BL21 cells harboring pET-IFN-γ alone or together with pGro7 were cultured overnight in Luria–Bertani medium at 37°C and 200 rpm with kanamycin (50 μg/ml) or together with chloramphenicol (20 μg/ml), respectively. To perform coexpression, the overnight cultured seed liquid was inoculated into 150 ml 2× YT medium containing antibiotics for plasmids selection and 0–0.6 g/L L-arabinose for induction of chaperonin GroEL/GroES. The cell growth of the recombinant *E. coli*

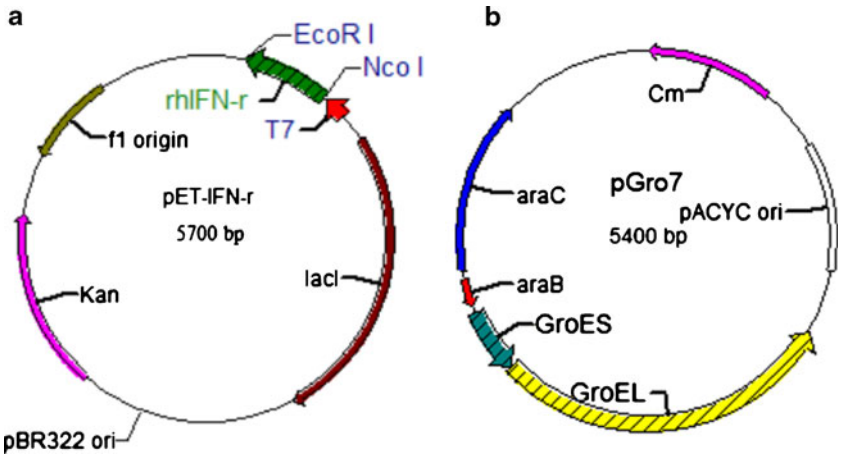

Fig. 1 Structure of the plasmids pET-IFN-γ and pGro7. **a** Plasmid pET-IFN-γ. **b** Plasmid pGro7

was calibrated by turbidity measurement at 600 nm using UltraSpec 3300pro spectrophotometer (GE Healthcare, USA). When the OD_{600} reached 0.6 (about 3 h), IPTG was added to induce the expression of rhIFN-γ. After further growth for 8 h, the cells were harvested by centrifugation at 10,000×*g* and 4°C for 10 min. The collected cells were suspended in phosphate-buffered saline (PBS) buffer (137 mM NaCl, 2.7 mM KCl, 10 mM Na_2HPO_4, and 2 mM KH_2PO_4, pH 7.4), and disrupted by ultrasonication. After centrifugation at 13,000×*g* and 4°C for 30 min, the precipitate was resuspended in PBS buffer, and the supernatant and precipitate were fractionated by sodium dodecyl sulfate polyacrylamide gel electrophoresis (SDS-PAGE) on 4–12% gradient stained with Coomassie brilliant blue G-250. The relative quantities of the protein bands on the gels were analyzed by gel documentation unit (BioRad, USA). Ni-NTA metal-affinity chromatography was used to purify the rhIFN-γ with the C-terminal six histidine tag according to the instruction manual (Bio Basic, Canada).

Spectra measurement

Far-UV circular dichroism (CD) measurements were performed on a MOS-450 spectropolarimeter (Bio-Logic, France). The spectra were recorded over 190–240 nm using a cuvette of 1 mm pathlength at a scan speed of 60 nm/min and a time constant of 1 s. The CD data were further processed for baseline subtraction, noise reduction, and signal averaging and presented as ellipticity (θ, millidegree). The secondary structure fractions were calculated from the CD spectra using CONTINLL method (Vanstokkum et al. 1990; Whitmore and Wallace 2008). The fluorescence spectra were measured with an F-4500 fluorescence spectrometer (Hitachi, Japan). The excitation wavelength was 295 nm, and the emission spectra were recorded from 300 to 450 nm. The recombinant human interferon-γ expressed in *E. coli* with a specific activity of 2×10^7 IU/mg was used as the standard (Bio Basic, Canada), of which the single non-glycosylated polypeptide chain is composed of 144 amino acids with a molecular weight of approximately 17 kDa.

Analytical size exclusion chromatography

Analytical size exclusion chromatography (SEC) was used to detect the active dimeric structure of rhIFN-γ. The experiment was performed on a TSK-GEL $G3000SW_{XL}$ column (Tosoh Bioscience, Japan) equilibrated with PBS buffer (pH 7.4) at a flow rate of 0.3 ml/min. Low molecular weight calibration kit (GE Healthcare, USA) was used as a reference containing phophorylase b (97 kDa), albumin (66 kDa), ovalbumin (45 kDa), carbonic anhydrase (30 kDa), trypsin inhibitor (20.1 kDa), and α-lactalbumin (14.4 kDa). The elution profile of the rhIFN-γ was compared with the standards for determining the molecular weight of the dimer and monomer.

Cross-linking analysis

The active dimeric structure of rhIFN-γ was further confirmed by interchain cross-linking using disuccinimidyl suberate (DSS) (Pierce, USA) (Reddy et al. 2007). For this reaction, 40 μl of purified rhIFN-γ and 10 μl DSS (25 mM in DMSO) were mixed, and the reaction mixture was incubated for 30 min at room temperature. The reaction was quenched by adding Tris to a final concentration of 20 mM for 15 min. The cross-linked dimer was analyzed by SDS-PAGE.

Enzyme-linked immunosorbent assay

The enzyme-linked immunosorbent assay (ELISA) assay for immunoreactivity of active rhIFN-γ was carried out with human IFN-gamma Platinum ELISA Kit (Bender MedSystems, Austria), where native hIFN-γ with a specific activity of 2×10^7 IU/mg was used as the standard. Firstly, the cell culture supernatant samples and reference were added to microwells coated with murine monoclonal

antibody to hIFN-γ. A biotin-conjugated anti-hIFN-γ monoclonal antibody was added to the microwells and bound to rhIFN-γ captured by the primary antibody after the incubation for 2 h at room temperature. Finally, streptavidin–horseradish peroxidase was added, and the microwells were again incubated for 1 h at the same temperature. The microwells should be completely rinsed with the wash buffer (PBS with 0.05% Tween 20) after each incubation. Following the second incubation, the substrate solution (tetramethyl-benzidine) was added, and the color reaction proceeded about 10 min. The reaction was terminated by adding the stop solution (1 M phosphoric acid), and the absorbance was read at 450 nm. According to the standard hIFN-γ dilutions, a calibration curve for hIFN-γ ELISA was drawn, and the active rhIFN-γ sample concentration was determined.

Yeast two-hybrid system

Matchmaker two-hybrid system 3 (Clontech, USA) was used as the transcriptional assay to investigate protein–protein interactions in vivo in yeast. Vectors of pGBKT7 and pACT2 were used as DNA-BD and AD fusion vectors, respectively. To generate the bait plasmids of pGBKT7-IFN-γ, pGBKT7-GroEL, and pGBKT7-GroES, herein the rhIFN-γ, GroEL and GroES genes were amplified using PCR. Amplified sequences were cloned into pGBKT7 between *Nco*I and *Eco*RI sites and thereby fused in-frame to the GAL4 DNA binding domain and the c-Myc epitope tag. Similarly to generate the prey plasmid pACT2-IFN-γ, the rhIFN-γ sequence was cloned into pACT2 between the *Nco*I and *Xho*I sites and thereby expressed as a fusion protein with the SV40 nuclear-localization signal, GAL4 transcription-activating domain and the HA epitope tag. *Saccharomyces cerevisiae* strains AH109 and Y187 were used as the hosts for the bait and prey plasmids, respectively. Plasmid DNA transformation was done by the lithium acetate (LiAc)-mediated method (Gietz et al. 1992), and yeast mating was applied to cotransform the bait and prey plasmids into yeast strain AH109 (Bendixen et al. 1994). Cells were grown in complete minimal medium lacking leucine or tryptophan to select for the presence of different plasmids and screened the protein–protein interactions by *HIS3* reporter gene expression.

Results

Changes in the growth profile of *E. coli* BL21 transformed with different plasmids

When host cells are programmed to produce large amounts of heterologous proteins, extra energy is required to synthesize relevant nucleic acids and proteins. The aggravated metabolic load imposed on the cells may adversely influence the host growth as well as the expression level of target proteins. To investigate the influence of coexpressing chaperonin on the host growth, the growth curves were determined for *E. coli* transformed stains expressing rhIFN-γ with or without GroEL/GroES (Fig. 2). At the initial phase, the growth curves for both the strains were almost overlapping. After induced at 2.5 h, the growth rate for pET-IFN-γ-pGro7 transformed cells was obviously higher than that for pET-IFN-γ only transformed cells. Fitting the exponential phase curves (Gupta et al. 2006), the specific growth rate constants (μ) for strains expressing rhIFN-γ with or without GroEL/GroES were obtained at 0.407 h^{-1} (R^2 was 0.9733) and 0.309 h^{-1} (R^2 was 0.9765), respectively. The results demonstrated that chaperonin GroEL/GroES coexpression could effectively accelerate the host growth owing to enhancing the folding efficiency of some essential *E. coli* proteins and reducing the toxicity of aggregates to the host cells (Gupta et al. 2006; Hartl and Hayer-Hartl 2002; Stefani and Dobson 2003). With the improved growth, the bacterial cells were able to supply more metabolic energy to support the soluble expression of rhIFN-γ.

Optimizing the temperature and inducer concentration yielded higher level of soluble rhIFN-γ

To investigate the effects of fermentation conditions on soluble expression, rhIFN-γ was produced at different culture temperature (37°C, 30°C, and 25°C) and IPTG concentration (the final concentration of 0.5, 0.2, and 0.1 mM), while the GroEL/GroES was induced with a

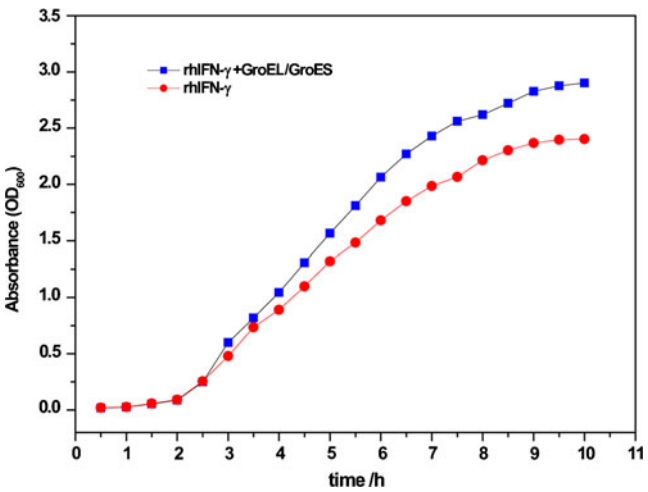

Fig. 2 Growth curves for recombinant *E. coli* BL21. *Solid squares* show the growth characteristic of strains expressing rhIFN-γ with the presence of GroEL/GroES. *Solid circles* show the growth characteristic of strains expressing rhIFN-γ only

constant amount of L-arabinose (the final concentration of 0.5 g/L). The *E. coli* BL21 transformed with pET-IFN-γ only was cultivated at 25°C as the control. The relative amount of rhIFN-γ at different conditions and SDS-PAGE of corresponding proteins in the supernatant and precipitate are shown in Fig. 3. According to the results, soluble rhIFN-γ expression at 37°C was both very low, no matter with or without chaperonin coexpression. However, when the temperature was decreased to 25°C, soluble rhIFN-γ expression level with chaperonin coexpression was greatly enhanced by 2.2 times compared with the control. In addition, the optimal IPTG concentration was 0.2 mM for the soluble expression of rhIFN-γ.

Effect of chaperonin GroEL/GroES on the soluble expression of rhIFN-γ

To study the effect of chaperonin on soluble rhIFN-γ expression, the GroEL/GroES induction was changed by adding different concentration of L-arabinose in the range of 0–0.6 g/L, while the rhIFN-γ expression was controlled by adding a constant amount of IPTG (the final concentration of 0.2 mM) cultured at 25°C. The generated GroEL shown in Fig. 4 exhibited a linear relationship to the amount of inducer L-arabinose at low concentration. With the increase of L-arabinose, the induction of GroEL/GroES was gradually saturated and the amount of chaperonin reached the equilibrium. Interestingly, there was a significantly positive correlation between the ratio of supernatant to precipitate of rhIFN-γ and the chaperonin level, indicating that chaperonin effectively promoted soluble rhIFN-γ expression. Unfortunately, the small amounts of inclusion bodies were still found even with the presence of high GroEL/GroES concentration, and similar phenomenon was also observed in the IFN-γ refolding assisted by GroEL/GroES in vitro (Vandenbroeck and Billiau 1998; Vandenbroeck et al. 1998).

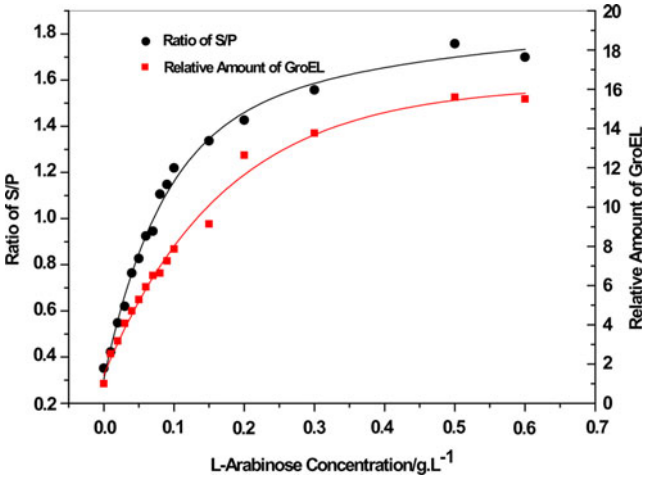

Fig. 4 Effect of L-arabinose concentration on GroEL and rhIFN-γ expression. *Solid squares* show the GroEL expression at different L-arabinose concentration. *Solid circles* show the ratio of supernatant to precipitate of rhIFN-γ at different L-arabinose concentration

Identification of rhIFN-γ by circular dichroism and fluorescence measurements

To be functionally active, the protein must fold to its unique steric structure. Here, we focused on the conformation of soluble rhIFN-γ using CD because it is a powerful conformational probe for the regular secondary structure in proteins. The CD spectra in the far-UV region (190–240 nm) were recorded to provide an estimation of the secondary structure composition of rhIFN-γ. From Fig. 5a, the positive values near the 192 nm, the negative values near the 206 and 220 nm on both the standard and soluble rhIFN-γ curves are in accordance with the characteristic of the α-helix conformation. Furthermore, the peaks near the 206 and 220 nm in both the standard rhIFN-γ and the soluble rhIFN-γ can fully identify their similar secondary structure. (Sharon et al. 2005). By analysis of the soluble rhIFN-γ curve, the fractions of several secondary structures

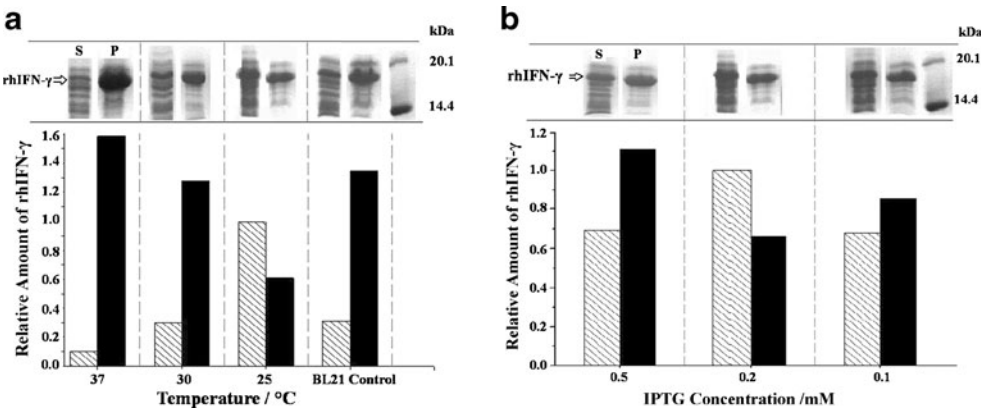

Fig. 3 SDS-PAGE of supernatant (*S*) and precipitate (*P*) fractions and relative amount of rhIFN-γ at different fermentation conditions. **a** Cultured at different temperatures and 0.2 mM IPTG concentration. **b** Cultured at different IPTG concentration and 25°C

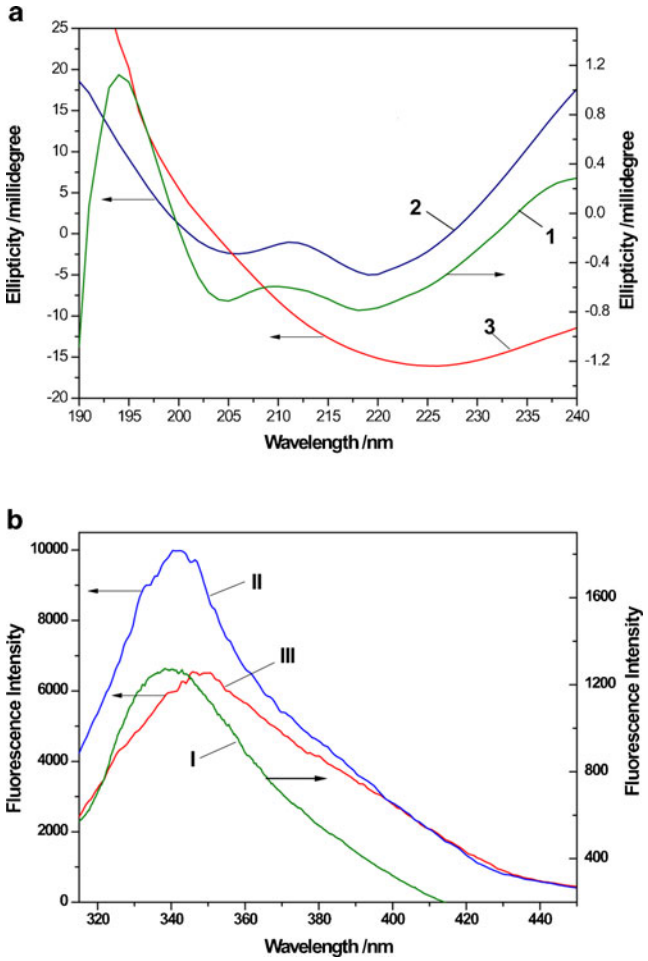

Fig. 5 Spectra analysis of rhIFN-γ structure. **a** CD spectra. *Curve 1* Standard rhIFN-γ; *curve 2* soluble rhIFN-γ; *curve 3* denatured rhIFN-γ. **b** Fluorescence spectra. *Curve I* Standard rhIFN-γ; *curve II* soluble rhIFN-γ; *curve III* denatured rhIFN-γ. The *arrows* indicate the respective *Y*-axis for each curve

were calculated through CONTINLL method. The results showed that soluble rhIFN-γ contained 40.9% α-helix, 9.8% β-strand, 28.2% β-turn, and 21.2% disordered and indicated that the tertiary structure of soluble rhIFN-γ was mainly built up from α-helices (Levitt and Chothia 1976), which was in accordance with the X-ray crystallography of rhIFN-γ (Ealick et al. 1991).

The fluorescence spectra also provide a meaningful insight into the conformational changes in proteins, since it can reflect the local environment changes around certain residues on the level of tertiary structure. When rhIFN-γ was excited at 295 nm, the observed spectra were regarded as the fluorescence emission of the unique tryptophan residue (Trp 38) (Tsaprailis et al. 1998). The maximum emission peak of soluble rhIFN-γ shown in Fig. 5b was nearly identical to that of standard rhIFN-γ around 340 nm, indicating no changes in the microenvironment of the unique tryptophan per subunit. As a contrast, the emission peak of denatured rhIFN-γ shifted from 340 to 350 nm, and the red shift suggested the polypeptide was unfolding accompanied by exposing its single tryptophan to the solvent.

Direct evidences for the dimeric structure of rhIFN-γ: size exclusion chromatography and cross-linking analysis

The single chain of rhIFN-γ with 6× His-tag has a molecular weight of 18 kDa, but the bioactive rhIFN-γ is considered to be a stable homodimer. SEC was used to detect the dimer and monomer for the quaternary structure of rhIFN-γ. From Fig. 6, the fractions eluted between ovalbumin (45 kDa) and carbonic anhydrase (30 kDa) denoted the dimer of rhIFN-γ with the molecular weight of approximately 36 kDa (peak 1), and the elution between trypsin inhibitor (20.1 kDa) and α-lactalbumin (14.4 kDa) was the monomer of approximately 18 kDa (peak 2). The soluble expression yielded more than 95% of the dimeric rhIFN-γ according to the HPLC data.

A further evidence for the dimer formation was obtained from the interchain cross-linking of the purified rhIFN-γ followed by SDS-PAGE (Fig. 7). A single band corresponding to ~36 kDa clearly indicated the formation of the properly assembled dimer. Moreover, it was found that most of the soluble rhIFN-γ adopted the dimeric configuration instead of a monomeric structure, which was coincident with the SEC results.

Immunoreactivity assay of rhIFN-γ by ELISA

ELISA method was taken to measure the immunoreactivity of the soluble rhIFN-γ. Since the immunoreactivity in ELISA exhibited a direct relationship with the dimer structure and biological activity (Vandenbroeck et al. 1998, 1993), the actual amount of bioactive rhIFN-γ could be conversed. The concentration of active rhIFN-γ calculated from the ELISA was 72.91 mg/L fermentation broth. Referring to the international NIBSC 82/587 Standard (1 IU corresponding to 50 pg hIFN-γ), equivalent of 1.46×10^9 IU/L rhIFN-γ was acquired through coexpressing the chaperonin GroEL/GroES in recombinant *E. coli*.

rhIFN-γ/chaperonin interactions

As an approach to identify molecular interactions that mediated the folding of rhIFN-γ in vivo, the yeast two-hybrid system was applied to know the functional role of chaperonin in the coexpression system and the existence of rhIFN-γ homodimer (Fig. 8). The bait and prey plasmids were cotransformed into strain AH109 and screened for interacting proteins by *HIS3* reporter gene. On the basis of results with the SD/–Leu/–Trp/–His assay, rhIFN-γ was

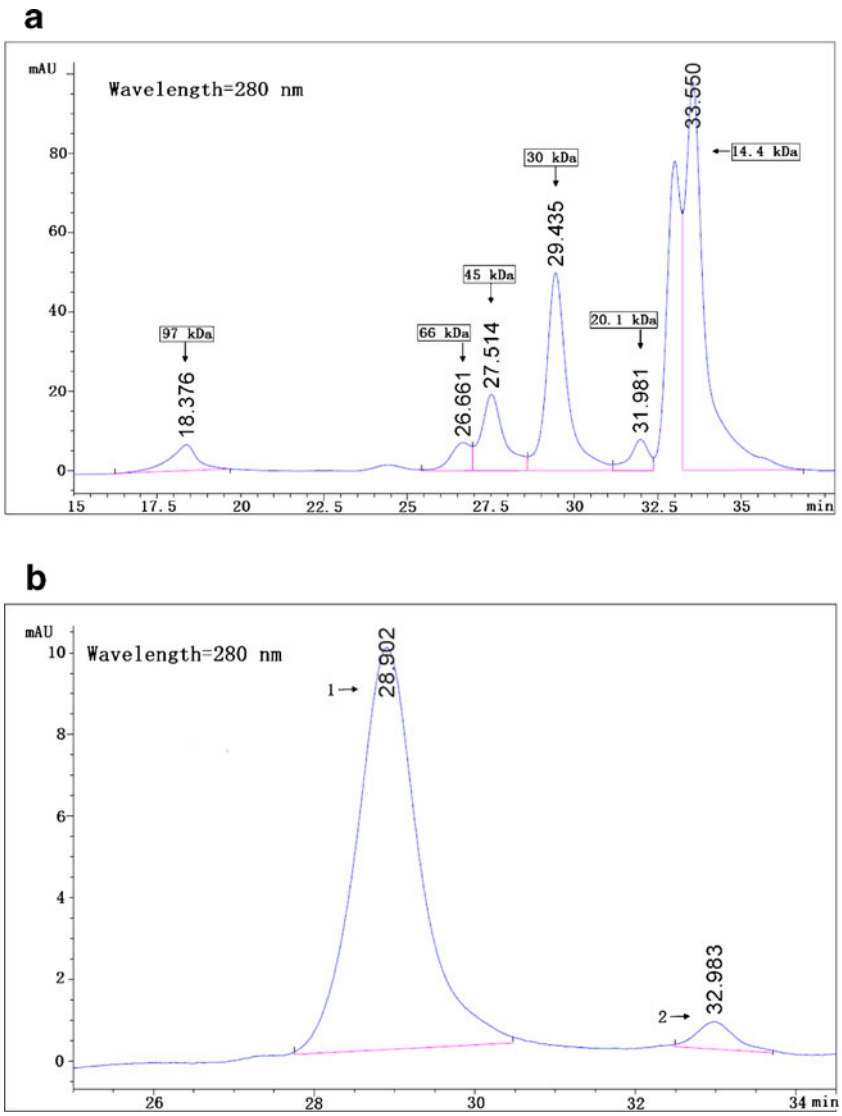

Fig. 6 The SEC profiles of protein standards and soluble rhIFN-γ with retention time showed above the peaks. **a** Standard proteins that contain phophorylase b (97 kDa), albumin (66 kDa), ovalbumin (45 kDa), carbonic anhydrase (30 kDa), trypsin inhibitor (20.1 kDa), and α-lactalbumin (14.4 kDa). **b** Soluble rhIFN-γ. *Peak 1* is the rhIFN-γ dimer with a mass of approximately 36 kDa, and *peak 2* represents the rhIFN-γ monomer with a mass of approximately 18 kDa

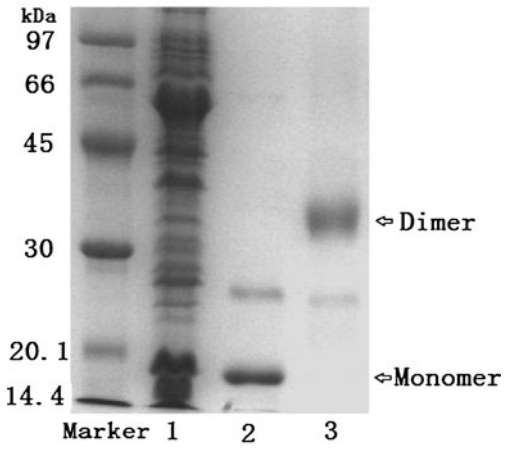

Fig. 7 SDS-PAGE analysis of cross-linked rhIFN-γ. *Lane 1* The whole cell supernatant; *lane 2* rhIFN-γ purified by one-step Ni-NTA metal-affinity chromatography; *lane 3* cross-linked rhIFN-γ

concluded to have a self-interaction (Fig. 8a), confirming the existence of the homodimeric rhIFN-γ. Importantly, GroES and GroEL were detected to have strong interactions with rhIFN-γ (Fig. 8b, c), which meant that chaperonins directly interacted with rhIFN-γ to increase its folding during the coexpression process.

Discussion

rhIFN-γ is a novel pharmaceutical protein in treating a series of diseases. Efficient production of active rhIFN-γ with less downstream steps is necessary. In this paper, we successfully achieved the soluble expression of rhIFN-γ through constructing a GroEL/GroES coexpression system in *E. coli*. The soluble rhIFN-γ effectively folded into a correct conformation that was identical to the native rhIFN-γ with the criteria such as secondary structure (CD

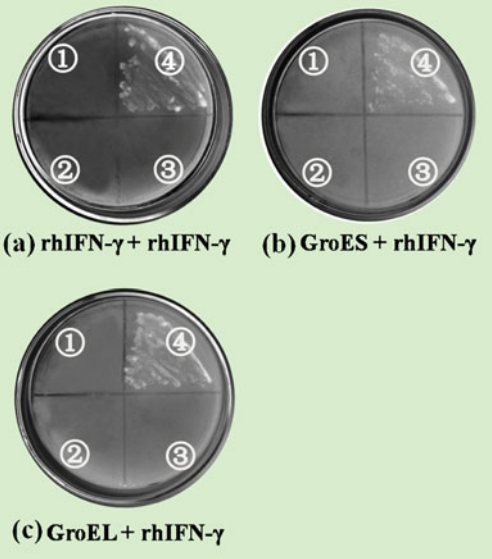

Fig. 8 Protein–protein interaction analysis using the yeast two-hybrid system. Bait and prey plasmids were constructed and representative interaction profiles between rhIFN-γ and rhIFN-γ, rhIFN-γ and GroES, and rhIFN-γ and GroEL are shown in **a**–**c**, respectively. In each culture plate, *zones 1–4* denote blank, bait plasmid, prey plasmid, and bait plasmid and prey plasmid, respectively

spectrum), tertiary structure (fluorescence spectrum), and quaternary structure (SEC and DSS cross-linking). Taking the ELISA assay for immunoreactivity, coexpressing chaperonin GroEL/GroES opened up a new opportunity for the production of active rhIFN-γ, and this improved expression system illustrated a good example for the production of other oligomeric proteins.

The yeast two-hybrid test (Fig. 8) and the positive relationship between the ratio of supernatant to precipitate of rhIFN-γ and the chaperonin level (Fig. 4) well proved that the GroEL/GroES interacted directly with rhIFN-γ to enhance its correct folding. In combination with the fact that the rhIFN-γ with the absence of chaperonin accumulated as aggregates even at a relatively low temperature (Fig. 3), we speculated the rhIFN-γ folded essentially via GroEL according to the following procedure. Firstly, the nascent rhIFN-γ chain exposing considerable hydrophobic amino acids was captured by GroEL via multiple interactions with hydrophobic surfaces on the apical GroEL domains. With GroES forming a lid on the GroEL cavity, the non-native rhIFN-γ was concerted released to an enclosed cage in which the protein was free to fold unimpaired by aggregation (Kerner et al. 2005). After folding in the cage for 10–15 s, the subunit was released to the cytoplasm with a structure closer to the native state. Due to the predominantly dimeric nature of rhIFN-γ, the subunit passing through chaperonin machinery still exposed substantial hydrophobic interfaces and was structurally unstable. Thus, both the rhIFN-γ subunit partially or totally of the native state would repeatedly return to GroEL for assisted folding or conformational maintenance (Houry et al. 1999). With the continuous assistance of the chaperonin GroEL/GroES, a large number of subunits had the opportunity of correctly assembling to the homodimer.

According to the putative folding process mentioned above, the strong temperature dependence of hydrophobic interactions among partially folding intermediates bore an unshirkable responsibility for rhIFN-γ aggregation. Thus, temperature played a crucial role in the soluble expression of rhIFN-γ. The nascent chains exposing their non-native features experienced a long period from translation to entrapping into the Anfinsen cage of GroEL/GroES system. At lower temperature (e.g., 25°C), the hydrophobic interactions were remarkably weakened; thus, a considerable number of intermediates were kept in a folding-competent state when they were captured by GroEL. With the assistance of GroEL/GroES system, the nonaggregated intermediates were finally correctly folded. Moreover, lower temperature is more favorable for GroEL/GroES to function efficiently. The protein folding and release activity of GroEL/GroES is gradually weakened due to a decreasing affinity of GroES for GroEL at non-permissive temperature (Gnoth et al. 2010; Goloubinoff et al. 1997).

One deficiency of the above GroEL/GroES coexpression system was that the inclusion bodies of rhIFN-γ seemed unavoidable even with the presence of high concentration of GroEL/GroES. Several reasons may account for that. Firstly, the chaperonin GroEL/GroES was sustainable not only for rhIFN-γ intermediates but also for a number of bacterial proteins and maintenance of cell viability during rhIFN-γ production process. At some particular moments, the concentration of folding intermediates could be very high, but the chaperonin binding sites were not available, resulting in the formation of inclusion bodies for those unassisted rhIFN-γ intermediates. Secondly, Vandenbroeck et al. demonstrated the dimerization of the folding-competent monomer was a rate-limiting step in the IFN-γ refolding process in vitro. For those monomer intermediates that had already passed through the GroEL/GroES machinery, the low solubility of this conformational state may form either aggregates (at high protein concentration and non-permissive temperature) or correctly assembled dimer (at low protein concentration and proper temperature). Once those thermal inactivation inclusion bodies occur, GroEL/GroES system cannot solubilize and refold them again according to the general concepts of GroEL/GroES action (Fenton and Horwich 1997). Therefore, the use of chaperone "cocktails" may become a prospective approach to avoid the inclusion bodies formation and yield a higher production. For example, trigger factor (TF), as a ribosome-binding chaperone, can bind to ribosomes and interact with nascent chains to stabilize them in a state competent for

subsequent folding. Chaperone system DnaK–DnaJ–GrpE acts on nascent chains subsequent to TF to keep the intermediates nonaggregated, and they can also act on protein aggregates to liberate and refold the polypeptides embedded inside the aggregates (Liberek et al. 2008; Moon et al. 2009). With the upstream control, GroEL/GroES system would ultimately exert a better function in the folding process.

Acknowledgements This work was financially supported by the National Natural Science Foundation of China (no. 20876138).

References

Bendixen C, Gangloff S, Rothstein R (1994) A yeast mating-selection scheme for detection of protein–protein interactions. Nucleic Acids Res 22:1778–1779

Blalock JE, Georgiades JA, Langford MP, Johnson HM (1980) Purified human immune interferon has more potent anticellular activity than fibroblast or leukocyte interferon. Cell Immunol 49:390–394

Brusehaber E, Schwiebs A, Schmidt M, Bottcher D, Bornscheuer UT (2010) Production of pig liver esterase in batch fermentation of *E. coli* Origami. Appl Microbiol Biotechnol 86:1337–1344

Contreras JAR, Pedraza-Reyes M, Ordonez LG, Estrada NU, de la Rosa APB, De Leon-Rodriguez A (2010) Replicative and integrative plasmids for production of human interferon gamma in *Bacillus subtilis*. Plasmid 64:170–176

Ealick SE, Cook WJ, Vijay-Kumar S, Carson M, Nagabhushan TL, Trotta PP, Bugg CE (1991) Three-dimensional structure of recombinant human interferon-gamma. Science 252:698–702

Ellerhorst JA, Kilbourn RG, Amato RJ, Zukiwski AA, Jones E, Logothetis CJ (1994) Phase-II trial of low-dose gamma-interferon in metastatic renal-cell carcinoma. J Urol 152:841–845

Fenton WA, Horwich AL (1997) GroEL-mediated protein folding. Protein Sci 6(4):743–760

Gao YG, Guan YX, Yao SJ, Cho MG (2003) On-column refolding of recombinant human interferon-gamma with an immobilized chaperone fragment. Biotechnol Prog 19:915–920

Giannopoulos A, Constantinides C, Fokaeas E, Stravodimos C, Giannopoulou M, Kyroudi A, Gounaris A (2003) The immunomodulating effect of interferon-γ intravesical instillations in preventing bladder cancer recurrence. Clin Cancer Res 9:5550–5558

Gietz D, St. Jean A, Woods RA, Schiestl RH (1992) Improved method for high efficiency transformation of intact yeast cells. Nucleic Acids Res 20:1425

Gnoth S, Simutis R, Lubbert A (2010) Selective expression of the soluble product fraction in *Escherichia coli* cultures employed in recombinant protein production processes. Appl Microbiol Biotechnol 87:2047–2058

Goloubinoff P, Diamant S, Weiss C, Azem A (1997) GroES binding regulates GroEL chaperonin activity under heat shock. FEBS Lett 407:215–219

Gray PW, Leung DW, Pennica D, Yelverton E, Najarian R, Simonsen CC, Derynck R, Sherwood PJ, Wallace DM, Berger SL (1982) Expression of human immune interferon cDNA in *E. coli* and monkey cells. Nature 295:503–508

Gupta P, Aggarwal N, Batra P, Mishra S, Chaudhuri TK (2006) Co-expression of chaperonin GroEL/GroES enhances in vivo folding of yeast mitochondrial aconitase and alters the growth characteristics of *Escherichia coli*. Int J Biochem Cell Biol 38:1975–1985

Hartl FU, Hayer-Hartl M (2002) Molecular chaperones in the cytosol: from nascent chain to folded protein. Science 295:1852–1858

Hernandez VEB, Maldonado L, Rivero EM, de la Rosa APB, Jimenez-Bremont JF, Acevedo LGO, Rodriguez ADL (2008) Periplasmic expression and recovery of human interferon gamma in *Escherichia coli*. Protein Expression Purif 59:169–174

Houry WA, Frishman D, Eckerskorn C, Lottspeich F, Hartl FU (1999) Identification of in vivo substrates of the chaperonin GroEL. Nature 402:147–154

Hsieh CA (2010) Expression and purification of recombinant human interferon-γ and interleukin-12 employing starch binding domain. Dissertation, National Tsing Hua University, Hsinchu City, Taiwan

Jin T, Guan YX, Yao SJ, Lin DQ, Cho MG (2006) On-column refolding of recombinant human interferon-γ inclusion bodies by expanded bed adsorption chromatography. Biotechnol Bioeng 93:755–760

Kerner MJ, Naylor DJ, Ishihama Y, Maier T, Chang HC, Stines AP, Georgopoulos C, Frishman D, Hayer-Hartl M, Mann M (2005) Proteome-wide analysis of chaperonin-dependent protein folding in *Escherichia coli*. Cell 122:209–220

Kim SY, Heo MA, Jeong YJ (2009) Improving the productivity of recombinant protein in *Escherichia coli* under thermal stress by coexpressing GroELS chaperone system. J Microbiol Biotechnol 19:72–77

Levitt M, Chothia C (1976) Structural patterns in globular proteins. Nature 261:552–558

Liberek K, Lewandowska A, Zietkiewicz S (2008) Chaperones in control of protein disaggregation. EMBO J 27:328–335

Marth C, Windbichler GH, Hausmaninger H, Petru E, Estermann K, Pelzer A, Mueller-Holzner E (2006) Interferon-gamma in combination with carboplatin and paclitaxel as a safe and effective first-line treatment option for advanced ovarian cancer: results of a phase I/II study. Int J Gynecol Cancer 16:1522–1528

Matsushita K, Takenouchi T, Shimada H, Tomonaga T, Hayashi H, Shioya A, Komatsu A, Matsubara H, Ochiai T (2006) Strong HLA-DR antigen expression on cancer cells relates to better prognosis of colorectal cancer patients: Possible involvement of c-myc suppression by interferon-gamma in situ. Cancer Sci 97:57–63

Miller CHT, Maher SG, Young HA (2009) Clinical use of interferon-γ. Ann NY Acad Sci 1182:69–79

Moon HJ, Jeya M, Yu IS, Ji JH, Oh DK, Lee JK (2009) Chaperone-aided expression of LipA and LplA followed by the increase in alpha-lipoic acid production. Appl Microbiol Biotechnol 83:329–337

Nishihara K, Kanemori M, Kitagawa M, Yanagi H, Yura T (1998) Chaperone coexpression plasmids: differential and synergistic roles of DnaK–DnaJ–GrpE and GroEL–GroES in assisting folding of an allergen of Japanese cedar pollen, Cryj2 in *Escherichia coli*. Appl Environ Microbiol 64:1694–1699

Parvez MK, Sehgal D, Sarin SK, Basir SF, Jameel S (2006) Inhibition of hepatitis B virus DNA replicative intermediate forms by recombinant interferon-gamma. World J Gastroenterol 12:3006–3014

Reddy PK, Reddy SG, Narala VR, Majee SS, Konda S, Gunwar S, Reddy RC (2007) Increased yield of high purity recombinant human interferon-gamma utilizing reversed phase column chromatography. Protein Expression Purif 52:123–130

Rubin BY, Gupta SL (1980) Differential efficacies of human type I and type II interferons as antiviral and antiproliferative agents. Proc Natl Acad Sci U S A 77:5928–5932

Sambrook J, Fritsch EF, Maniatis T (1989) Molecular cloning: a laboratory manual. Cold Spring Harbor Laboratory Press, New York

Schoenborn JR, Wilson CB (2007) Regulation of interferon-gamma during innate and adaptive immune responses. Adv Immunol 96:41–101

Sharon MK, Thomas JJ, Nicholas CP (2005) How to study proteins by circular dichroism. Biochim Biophys Acta 1751:119–139

Sigidin YA, Loukina GV, Skurkovich B, Skurkovich S (2001) Randomized, double-blind trial of anti-interferon-gamma antibodies in rheumatoid arthritis. Scand J Rheumatol Suppl 30:203–207

Stefani M, Dobson CM (2003) Protein aggregation and aggregate toxicity: new insights into protein folding, misfolding diseases and biological evolution. J Mol Med 81:678–699

Suárez-Méndez R, García-García I, Fernández-Olivera N, Valdés-Quintana M, Milanés-Virelles MT, Carbonell D, Machado-Molina D, Valenzuela-Silva CM, López-Saura PA (2004) Adjuvant interferon gamma in patients with drug-resistant pulmonary tuberculosis: a pilot study. BMC Infect Dis 4:44

Tsaprailis G, Chan DWS, English AM (1998) Conformational states in denaturants of cytochrome c and horseradish peroxidases examined by fluorescence and circular dichroism. Biochemistry 37:2004–2016

Vandenbroeck K, Billiau A (1998) Interferon-gamma is a target for binding and folding by both *Escherichia coli* chaperone model systems GroEL/GroES and DnaK/DnaJ/GrpE. Biochimie 80:729–737

Vandenbroeck K, Martens E, Dandrea S, Billiau A (1993) Refolding and single-step purification of porcine interferon-gamma from *Escherichia coli* inclusion bodies. Eur J Biochem 215:481–486

Vandenbroeck K, Martens E, Billiau A (1998) GroEL/ES chaperonins protect interferon-gamma against physicochemical stress–study of tertiary structure formation by alpha-casein quenching and ELISA. Eur J Biochem 251:181–188

Vanstokkum IHM, Spoelder HJW, Bloemendal M, Vangrondelle R, Groen FCA (1990) Estimation of protein secondary structure and error analysis from circular-dichroism spectra. Anal Biochem 191:110–118

Whitmore L, Wallace BA (2008) Protein secondary structure analyses from circular dichroism spectroscopy: methods and reference databases. Biopolymers 89:392–400

Zhang Z, Tong KT, Belew M, Pettersson T, Janson JC (1992) Production, purification and characterization of recombinant human interferon-gamma. J Chromatogr A 604:143–155